ACS Sustainable Chemistry & Engineering

pubs.acs.org/journal/ascecg

Research Article

Rewritable Polymer Films Based on Topo-Polymerization of Diacetylenes in Poly(Propylene Carbonate)

Zhenni Zhou, Wei Wei, Song Li, Yue Zhang, Qingying Yao, Mingli Ni,* Haiyan Peng,* Xingping Zhou, and Xiaolin Xie

Cite This: *ACS Sustainable Chem. Eng.* 2021, 9, 5902−5909

Read Online

ACCESS | Metrics & More | Article Recommendations | Supporting Information

ABSTRACT: Photopatterning on polymer films has attracted extensive attention due to its widespread applications. Nevertheless, it is still challenging to rewrite these patterns. Herein, we demonstrate a viable approach toward the rewritable polymer films based on topo-polymerization of the diacetylene monomer (e.g., 10, 12-pentacosadiynoic acid, PCDA) in poly(propylene carbonate) (i.e., PPC). Rewritability of at least 17 times through the reversible colorimetric change of polydiacetylene (PDA) is achieved, and the written information can be maintained for 9 months under ambient conditions. Moreover, it is found that the hydrogen bonding interaction between PCDA and PPC plays a key role in improving the rewriting performance according to variable temperature Fourier transform infrared spectroscopy and molecular dynamics simulations. Well-defined assembly of PCDA along the PPC main chain is enabled, which leads to improved topo-polymerization of PCDA. The proposed paradigm here paves the way to design rewritable polymer films with customized patterning.

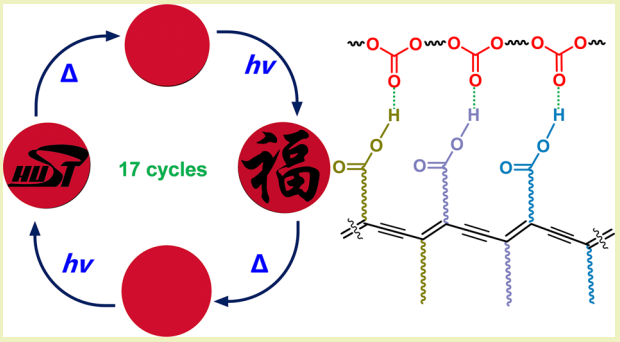

KEYWORDS: *photopatterning, rewriting, poly(propylene carbonate), diacetylene, hydrogen bonding, topo-polymerization, topochemical polymerization*

INTRODUCTION

Photopatterning on polymer films has garnered considerable attention due to the widespread applications such as surface functionalization, packaging, advertising, anticounterfeiting, and other advanced optical applications.[1−6] However, these patterns are generally difficult to rewrite.

As a solution, it would be reasonable to integrate the polymer film with responsive materials that are capable of changing colors upon external stimuli (e.g., light, temperature, pH, and humidity).[7−14] In this regard, polydiacetylene (PDA), which was pioneered by Wegner in 1969,[15] has drawn particular attention because of its reversible colorimetric transition between the red and blue colors in response to heating or light irradiation,[16−25] given that PDA is typically obtained through topo-polymerization of the diacetylene monomers. In general, PDA is blue in color due to the boosted π-conjugation and red shift in the ultraviolet−visible (UV−vis) absorption to the red and green light regions.[15,16,25] The chromatic transition of PDA is owing to the conformational switch. For instance, PDA changes from blue to red color upon stimuli such as heating due to which the fluctuations of the side chains lead to distortions of the main chains, decrease in the effective conjugation length, and a blue shift of UV−vis absorption.[17,21,26] In some cases, the color recovers when the stimuli is removed[21,22,27] or when exposed to UV light[16] because the chains restore their original confirmations. Despite the well-defined assemblies of diacetylene monomers through physical vapor transport for single crystal electronic devices,[28] it still remains a challenge to achieve robust colorimetric reversibility of PDA in a polymer film via assembly control.[22,27,29]

Blending a polymer with the diacetylene monomer is a rational way toward the rewritable polymer film. Jelinek and co-workers achieved rewritable polymer films by blending the diacetylene monomer named 10,12-tricosadiynoic acid with poly(methyl methacrylate) and subsequent topo-polymerization.[16] They found that the red PDA could revert to blue upon UV irradiation. However, the color change is not fully reversible as the blue color film could change to red upon heating, but the red color film changes to purple rather than blue upon UV light irradiation. The lack of strong interactions would lead to incomplete reversibility.

Hydrogen bonding interaction has been proven to be critical for the reversibility of colorimetric transition.[21,27,30] Increasing

Received: January 9, 2021
Revised: March 10, 2021
Published: April 22, 2021

https://doi.org/10.1021/acssuschemeng.1c00181
ACS Sustainable Chem. Eng. 2021, 9, 5902−5909

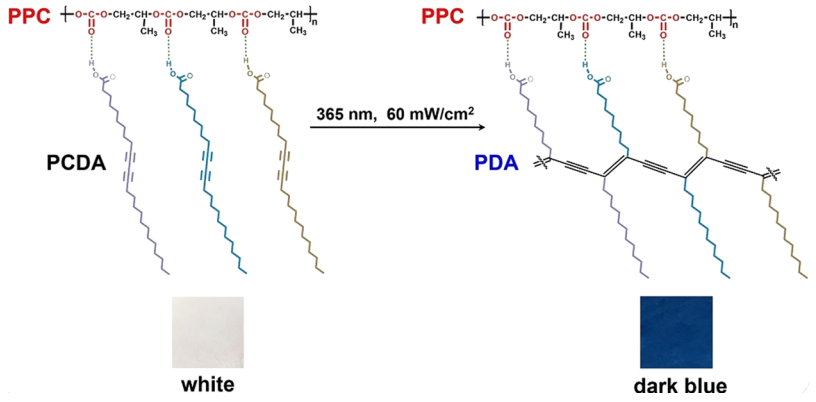

Figure 1. Schematic illustration of the unique assembly and topo-polymerization of PCDA in PPC, giving rise to color change from white to dark blue under room light.

the hydrogen bonding interactions between the polymer and diacetylene monomer could promote the assembly and topo-polymerization of diacetylene. To do this, Killops and co-workers employed poly(styrene-*b*-acrylic acid) as the template to induce the assembly of imidazolyl diphenyl-diacetylene monomers, achieving the greatly promoted topo-polymerization of the diacetylene monomer.[30] However, the rewriting capability is unexplored. With inspiration from this work, herein, we propose a viable approach for designing rewritable polymer films (thickness: 100 μm) by controlling the assembly of the diacetylene monomer (e.g., 10,12-pentacosadiynoic acid, PCDA) in poly(propylene carbonate) (i.e., PPC). PPC possesses plenty of carbonate groups to form hydrogen bonds with PCDA. The results demonstrated that well-defined assembly of PCDA occurred in the presence of PPC, leading to remarkable conversion of PCDA to PDA through topo-polymerization. In addition, due to the enhanced hydrogen bonding interactions between PDA and PPC, the reversible colorimetric change of PDA can be reproduced at least 17 times, and the written information can be maintained for 9 months under ambient conditions. Furthermore, a dramatically synergistic increase in the thermochromic transition temperature of PDA and thermal resistance of PPC was achieved. Lastly, the use of PPC is beneficial since PPC is an emerging sustainable and biodegradable polymer.[31−34]

RESULTS AND DISCUSSION

Writing and Erasing in the Rewritable Polymer Film.

Our concept of rewritable polymer films is realized based on the controlled assembly and subsequent topo-polymerization of PCDA in the presence of PPC. We surmised that the hydrogen bonding interactions between the carbonate groups of PPC and the carboxylic acid head groups of PCDA could lead to a well-defined assembly and remarkable topo-polymerization of PCDA along with the PPC main chain (Figure 1). Experiments show that the topo-polymerization can be completed within 60 s in CH_2Cl_2 and within 20 s in solid upon exposure to 60 mW/cm^2 of 365 nm light, giving rise to a color change from white to dark blue under room light. The topo-polymerization could even occur when exposing the PPC/PCDA film to room light for 24 h (Figure S1). However, no polymerization of PCDA took place in poly(butylene succinate) (PBS) when exposed to room light, despite the existence of carbonyl groups in the PBS main chain that could form hydrogen bonds with PCDA. In addition, no polymerization was observed when mixing PCDA with PBS in CH_2Cl_2, even under exposure to 60 mW/cm^2 of 365 nm light irradiation (Figure S2). In addition, polymers such as poly(vinyl acetate) (i.e., PVAc), poly(methyl methacrylate) (i.e., PMMA), and bisphenol A polycarbonate (i.e., BAPC) with fewer hydrogen bonding interactions with PCDA make it difficult to promote the topo-polymerization of PCDA in organic solvents such as acetone and CH_2Cl_2. These results suggest that PPC can induce a unique assembly of PCDA, consequently leading to the enhanced topo-polymerization.

The robust rewriting capabilities of our rewritable polymer films were also demonstrated. As shown in Figure 2a, the blue

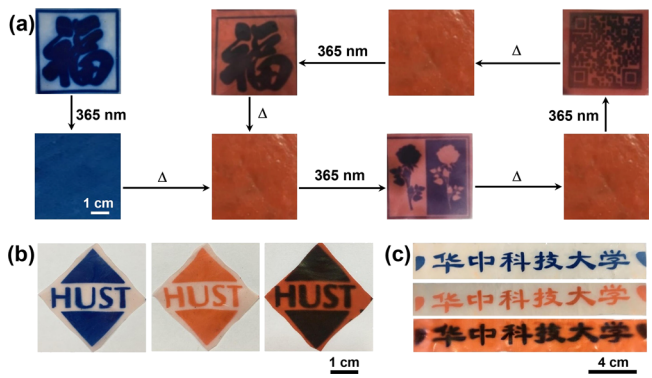

Figure 2. (a) Experimental results of (re)writing by UV light irradiation (365 nm, 60 mW/cm^2) through photomasks and erasing by heating (110 °C). (b) English abbreviation and (c) Chinese version of HUST written on the rewritable polymer films in different colors.

colored Chinese letter "fu" meaning best wishes can be written in the white PCDA/PPC film (thickness: 100 μm) upon exposure to 60 mW/cm^2 of 365 nm light irradiation through a photomask. Then, the written information can be erased by flood UV exposure, giving rise to a polymer film in dark blue. Upon heating to 110 °C for several seconds, the dark blue polymer film turns to bright red due to the absorption shift from 640 nm (excitonic) and 590 nm (vibronic) to 550 and 500 nm, respectively,[17] which can be rewritten by UV irradiation through a photomask due to the reversible absorption shift (Figure S3). The writing under UV irradiation and erasing upon heating are fully reversible and can be repeated at least 17 times without noticeable degradation (Figure S4). In contrast, the pristine PDA and PBS/PDA can be only rewritten eight and four times, respectively, although a low light intensity (40 mW/cm^2) was used to decrease the side photothermal effect when rewriting (Figure S5). The outstanding rewriting performance of the

https://doi.org/10.1021/acssuschemeng.1c00181
ACS Sustainable Chem. Eng. 2021, 9, 5902−5909

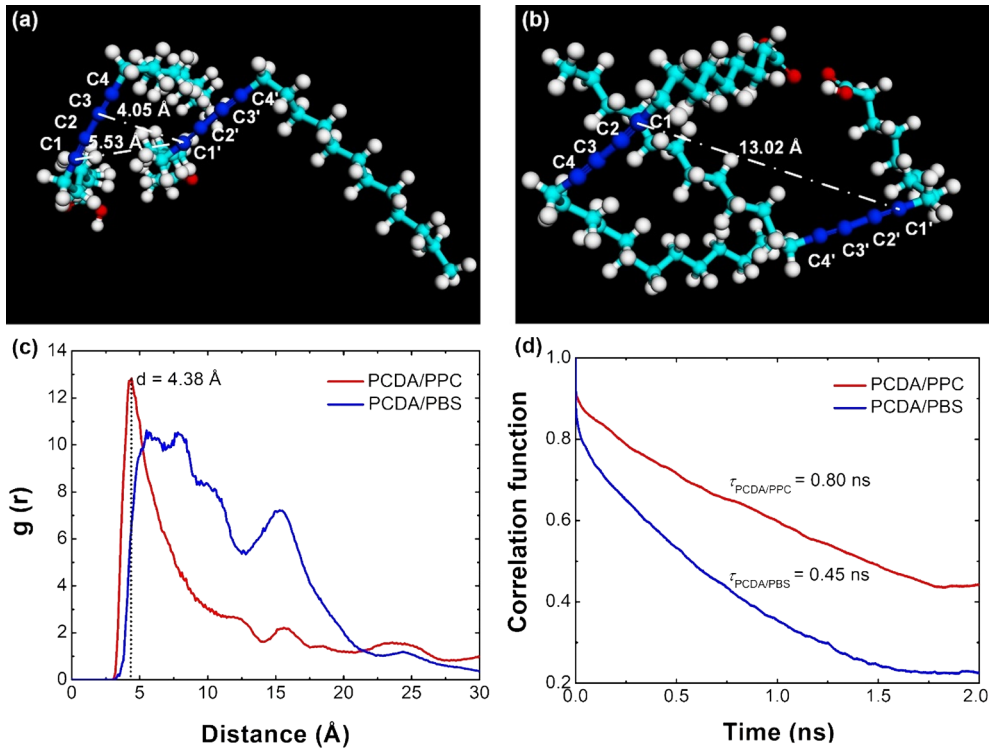

Figure 3. Molecular dynamics simulations. Snapshots of the equilibrated assembly of PCDA in (a) PPC and (b) PBS with CH_2Cl_2 as the solvent. PPC, PBS, and CH_2Cl_2 molecules are not displayed for clarity. (c) Radial distribution functions (g(r)) of the mass center of the diacetylene moiety. (d) Correlation function against time of the hydrogen bonds formed between PCDA and PPC or PBS from which the lifetime of hydrogen bonds can be obtained.

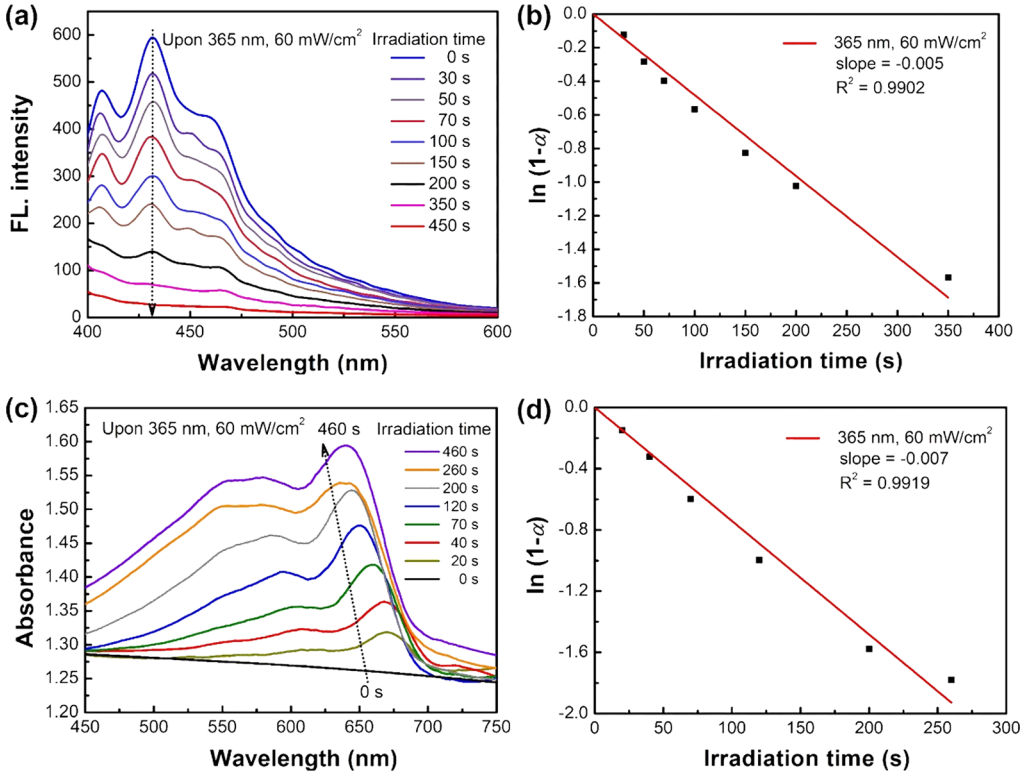

Figure 4. Topo-polymerization kinetics of PCDA in PPC. (a) Fluorescence (FL) intensity change and (b) kinetics fitting of the PCDA/PPC (1:10 by weight) film upon exposure to 60 mW/cm^2 of 365 nm light irradiation. (c) Visible absorption change and (d) kinetics fitting of the PCDA/PPC (1:10 by weight) film upon exposure to 60 mW/cm^2 of 365 nm light irradiation. The film thickness was 100 μm.

https://doi.org/10.1021/acssuschemeng.1c00181
ACS Sustainable Chem. Eng. 2021, 9, 5902−5909

PPC/PDA film could be owing to the hydrogen bonding interactions between PPC and PDA that facilitate the recovery of chain conformations of PDA.

Moreover, the information written in the rewritable PDA/PPC films can be customized (e.g., letters, images, and QR codes) by using different photomasks (Figure 2a), which can be also maintained for 9 months under ambient conditions. Considering the lifetime of the written information, our rewritable PDA/PPC polymer film exhibits excellent performance compared to other colorimetric materials (Table S1). Lastly, different colored information can be achieved by precisely controlling the writing process (Figure 2b,c). Dark blue letters and patterns can be written in the white PCDA/PPC film with a photomask under UV light exposure, associated with the conversion of PCDA to PDA through topo-polymerization. The dark blue letters and patterns can turn to bright red upon heating and other parts remain white. Dark blue letters and patterns can be also written in the bright red film upon UV irradiation.

Demonstration of Hydrogen Bonding Interactions. Molecular dynamics (MD) simulations demonstrated that the well-defined assembly of PCDA in PPC was enabled by the unique hydrogen bonding interactions. Figure 3a,b displays the snapshots of the equilibrated assembly of PCDA in PPC and PBS with CH_2Cl_2 as the solvent, respectively. The close stacking of PCDA molecules in the presence of PPC gives rise to a C1−C1′ distance of 5.53 Å between the adjacent two diacetylene moieties according to MD simulations, which is close to the ideal spatial parameter (5.0 Å) for topochemical polymerization.[35] On the contrary, a long C1−C1′ distance (13.02 Å) between the adjacent two diacetylene moieties explained why no PCDA polymerization occurred in the presence of PBS in CH_2Cl_2. The radial distribution functions of the mass center of the diacetylene moiety further confirmed the close stacking of PCDA in PPC (Figure 3c). A peak distance of 4.38 Å between the two diacetylene moieties in PPC is perfectly located in the range of 3.0−5.0 Å that is required for satisfactory topo-polymerization.[36,37] On the contrary, a disordered stacking of PCDA is noticed in PBS. The ordered assembly of PCDA in PPC can be attributed to the stronger hydrogen bonding interactions between PCDA and PPC, which is also supported by the longer hydrogen bonding lifetime in PPC than PBS (0.80 ns vs 0.45 ns, Figure 3d). Variable temperature Fourier transform infrared (FTIR) spectra experimentally prove a stronger hydrogen bonding interaction between PCDA and PPC. The peak associated with the C═O stretching of PPC in PPC/PCDA (1:1 by weight) shifts from 1745 to 1747 cm^{-1} when heated from 20 to 120 °C, due to which the hydrogen bonding interaction is weakened[38] (Figure S6a). In contrast, the C═O signal at 1714 cm^{-1} of PBS in the PBS/PCDA (1:1 by weight) film remains almost unchanged (Figure S6b). These results are in consistence with the MD simulations.

Polymerization Kinetics. Topo-polymerization kinetics measured with both fluorescence and UV−vis spectra reveals that the well-defined assembly of PCDA in PPC owing to the enhanced hydrogen bonding interactions is beneficial for topo-polymerization. It was found that the fluorescence intensity of the PCDA/PPC film linearly depended on the PCDA concentration, which could be quenched upon polymerization (Figures S7 and S8). Therefore, the topo-polymerization kinetics can be obtained by tracking the fluorescence quenching against the exposure time. As illustrated in Figure 4a, the fluorescence peaks of PCDA in PPC at 433 and 406 nm continuously decline with an increase in the exposure time. The conversion of PCDA reaches 95.5% upon irradiation for 450 s according to the fluorescence spectra. The Raman spectrum also shows that there is almost no residual PCDA monomer after flood UV exposure (Figure S9). Two strong peaks at 1455 and 2080 cm^{-1} which correspond to the ene−yne bond of PDA and a negligible peak at 2262 cm^{-1} that corresponds to the yne−yne bond of PCDA[29] indicate a full conversion of the PCDA monomer. The topo-polymerization of diacetylene monomers can be described using the first-order kinetics equation,[39]

$$\ln(1 - \alpha) = -kt \quad (1)$$

where, α is the PCDA conversion, k is the rate constant, and t is the irradiation time. As shown in Figure 4b, the experimentally determined kinetics agrees well with the theoretical prediction from which a rate constant of 0.005 s^{-1} is derived. Similarly, the topo-polymerization kinetics can be also obtained by monitoring the visible absorption change according to the Beer−Lambert law (Figure 4c). The appearance of the excitonic peak absorption at 640 nm in the UV−vis spectra with a vibronic maximum absorption at 590 nm is a sign of the conversion of PCDA to PDA through topo-polymerization.[17] A rate constant of 0.007 s^{-1} is calculated according to the increased absorption at 640 nm after complete polymerization (Figure 4d), which agrees well with the results from fluorescence quenching. In addition, it was found that the irradiation with higher light intensities favored the reaction rates (e.g., 0.016 and 0.027 s^{-1} under 80 and 100 mW/cm^2 of 365 nm irradiation, respectively), which increased the data deviations due to the photothermal effect (Figures S10 and S11). In general, similar to the topochemical polymerizations of dienes or trienes,[35] the topo-polymerization of PCDA is observed to obey the first-order reaction kinetics, which can be precisely controlled by tuning the light intensity.

Thermochromic Transition Temperature. Yang and coworkers proved that the PDA-based composite showed a higher reversible thermochromic transition temperature because of strong interactions.[17] In this work, the strong hydrogen bonding interactions between PDA and PPC also result in an increase in the thermochromic transition temperature. As illustrated in Figure 5, the pristine PDA shows a thermochromic transition from blue to red at 60 °C, similar to PDA/PBS, PDA/PVAc, PDA/PMMA, and PDA/BAPC films. In contrast, the thermochromic transition temperature of the PDA/PPC film is dramatically increased by 50% to 90 °C. The color change from dark blue to bright red of PDA/PPC was completed at 110

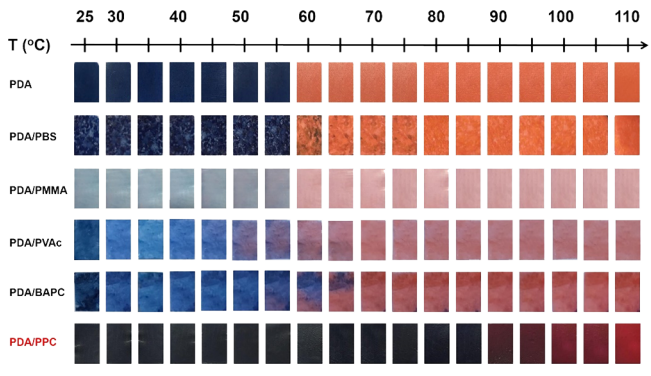

Figure 5. Thermochromic response and color transition temperatures of PDA in different polymer films.

https://doi.org/10.1021/acssuschemeng.1c00181
ACS Sustainable Chem. Eng. 2021, 9, 5902−5909

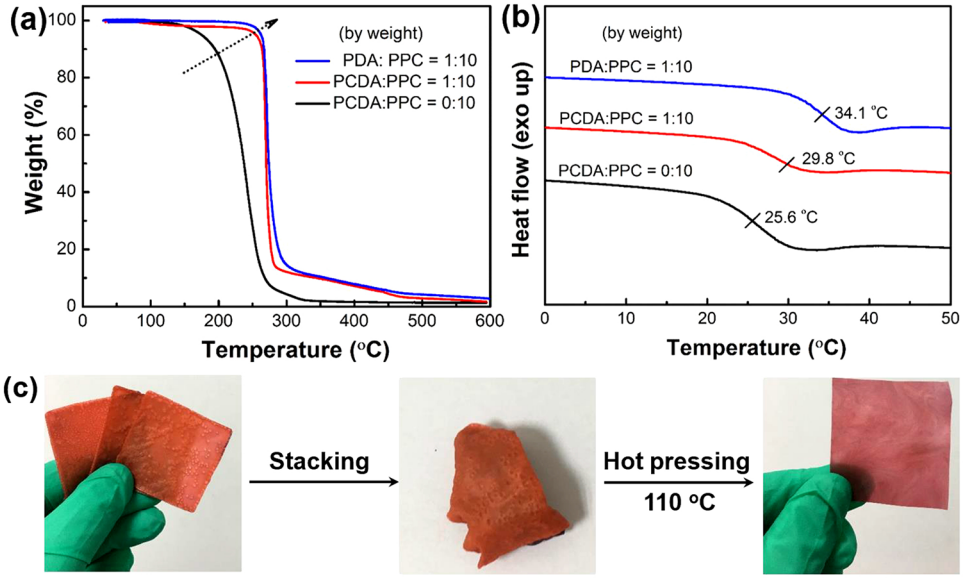

Figure 6. Effect of PCDA and PDA on (a) thermal stability and (b) glass transition temperatures of PPC films. (c) Recycling of the used PDA/PPC (1:10 by weight) film through simple hot-pressing.

°C. Such a high thermochromic transition temperature ensures a long lifetime of the written information in our rewritable polymer film at room temperature.

Thermal Stability and Glass Transition Behaviors. The thermal stability of PPC was also improved by the enhanced hydrogen bonding interactions. As illustrated in Figure 6a, the PCDA/PPC and PDA/PPC (1:10 by weight) films show an initial decomposition temperature of 262 °C (corresponding to 5% of weight loss), which is increased by 49.7% compared with that of the pristine PPC (175 °C). The glass transition temperatures (T_g) of PPC is also increased by 16.4% and 33.2% from 25.6 °C in the presence of PCDA and PDA, respectively (Figure 6b), indicating an increase in the confinement on the segment movement of PPC associated with the PCDA's topo-polymerization. No significant variation in the T_g is observed when changing the weight percentage of PDA (Figure S12). The addition of PCDA imposes a negligible impact on the thermal properties of PBS either (Figure S13). Therefore, given the attractive thermal properties, the used PDA/PPC polymer film can be recycled by simple hot-pressing at 110 °C with the information erased, as displayed in Figure 6c.

CONCLUSIONS

In summary, we demonstrated an approach toward rewritable polymer films with robust rewriting capabilities based on topo-polymerization of PCDA in PPC. The writing upon UV irradiation and erasing upon heating were reversible at least 17 times and the written information could be maintained for 9 months. The 50% increased thermochromic transition temperature greatly enhanced the stability of the written information. In addition, the initial decomposition temperature and glass transition temperature of PPC was increased by 49.7% and up to 33.2%, respectively. The high-performing rewritable polymer film was enabled by the unique assembly of PCDA in PPC through the remarkable hydrogen bonding interactions and the consequent promoted topo-polymerization as witnessed by MD simulations and variable temperature FTIR spectra. The reported rewritable polymer films in this work show a great application potential in writable labels, tags, packaging films, posters, and exhibition boards.

EXPERIMENTAL SECTION

Materials. PCDA (purity: >98%) was purchased from Alfa Aesar Co. Ltd., China. Before use, PCDA was purified through sequential dissolution in dichloromethane (CH_2Cl_2, DCM), filtration, and vacuum drying. PPC (M_n = 1.7 × 10^5) was supplied by Taizhou Bangfeng Plastic Co. Ltd., China. Prior to use, PPC was purified as follows: (1) dissolved in tetrahydrofuran (THF), (2) added dropwise into methyl alcohol to get the PPC precipitate, (3) washed with deionized water for five times, (4) filtered, and (5) dried under vacuum. All other reagents were used as-received without further purification. PMMA (M_n = 1.6 × 10^5) and PVAc (M_n = 5.0 × 10^4) were purchased from Alfa Aesar. PBS (M_n = 1.4 × 10^5) was supplied by Xinjiang Lanshan Tunhe Polyester Co. Ltd., China. BAPC (M_n = 3.3 × 10^4) was provided by Chimei Corporation, China. PMMA, PVAc, BAPC, and PBS were used as the control for PPC.

Characterization. UV−vis absorptions were characterized on a UV−vis spectrometer (UV-2600, Shimadzu, Japan). Variable temperature FTIR analysis was conducted on a FTIR spectrometer (Nexus 6700, Thermo Nicolet, United States) with temperature control accessories. Fluorescence spectra were excited by 377 nm (the maximum peak in the excitation spectra) irradiation and captured on a spectrofluorophotometer (RF-5301PC, Shimadzu, Japan). Raman spectra were recorded by a Raman spectrometer (HR800, HORIBA Jobin Yvon, France) with a 785 nm laser source. Differential scanning calorimetry (DSC) was performed on a DSC setup (Q2000, TA Instruments, United States) at a ramp rate of 10 °C/min from −30 to 100 °C. Dry nitrogen gas was continuously purged at a rate of 50 mL/min during the analysis. Thermogravimetric analysis (TGA) was performed on a TGA setup (TGA 4000, PerkinElmer, United States), and the sample was heated from 30 to 800 °C at a ramp rate of 10 °C/min under the protection of nitrogen gas. The photothermal effect was evaluated using a thermal imaging system (MAG32, Magnity Electronics Co. Ltd., China).

Molecular Dynamics Simulation. *Force Field.* All-atom force field parameters for PCDA, PPC, and PBS were adapted from the optimized potentials for liquid simulations (OPLS) force field.[40] The van der Waals parameters of DCM were directly taken from the general Amber force field (GAFF)[41] by the Automated Topology Builder (ATB).[42] The atomic partial charges of all molecules were derived by fitting the ab initio electrostatic potentials from Gaussian09[43] at the

https://doi.org/10.1021/acssuschemeng.1c00181
ACS Sustainable Chem. Eng. 2021, 9, 5902−5909

B3LYP/6-31G(d) level by the RESP scheme using AmberTools.[44] All force field parameters were validated to reproduce the experimentally measured density within a 5% deviation.

Simulation Details. MD simulations of PCDA/PPC/DCM and PCDA/PBS/DCM mixtures were carried out by the MD package GROMACS 4.6.7,[45] respectively. Since the cutoff should be less than half of the simulation box length, a 1.2 nm cutoff was optimized for computing both the van der Waals and electrostatic interactions. The long-range electrostatic interactions were computed by the particle mesh Ewald (PME) algorithm[46] in GROMACS 4.6.7. The periodic boundary condition (PBC) was applied in three dimensions. The equilibrated box length was within 6−7 nm. The mass ratio of PCDA to PPC or PBS was fixed at 1:10, in accordance with experiments. Thus, 10 PCDA and 70 PPC molecules were added into the PCDA/PPC/DCM mixture during computation, and 10 PCDA and 40 PBS molecules were added into the PCDA/PBS/DCM mixture, respectively; 3000 DCM molecules were added in each mixture. As previously reported,[47] when the number of repeating units equaled 5, the radial distribution function (RDF) was close to that with a larger number of repeating units. Thus, the number of repeating units of PPC and PBS was set to be 5 in the simulation to save the computation resources without significantly sacrificing the accuracy. To reach the dynamic equilibrium, the systems were annealed from 900 to 300 K for 10 ns with a time step of 1 fs and then maintained at 300 K in the *NPT* (*N*−conserved moles, *P*−pressure, and *T*−temperature) ensemble for 40 ns. The trajectory was saved every 1 ps for computing the RDF and hydrogen bonding lifetime. The existence of hydrogen bonds was determined by the distance r between the hydrogen donor and acceptor. When $r \leq r_{HB}$, the hydrogen bonding interaction was significant. With respect to the C═O···H−O hydrogen bond, r_{HB} equaled 0.35 nm, which was determined by the first minimum of the RDF.

Hydrogen Bonding Lifetime. The lifetime of hydrogen bonds was calculated from the averaged autocorrelation function of the existing functions of all hydrogen bonds,[48]

$$C(\tau) = \frac{\langle s_i(t) s_i(t+\tau)\rangle}{\langle s_i(t)^2\rangle} \quad (2)$$

with $s_i = \{0,1\}$ for the hydrogen bond i at time t. The integral of $C(\tau)$ provided a rough estimation of the average hydrogen bonding lifetime, τ_{HB},

$$\tau_{HB} = \int_0^\infty C(\tau)\,d\tau \quad (3)$$

Formulation. Typically, 50 mg PCDA and 500 mg PPC were dissolved in 20 mL CH_2Cl_2 under magnetic stirring for 18 h. Then, the solution was added dropwise into a polytetrafluoroethylene (PTFE) mold (4 cm × 4 cm × 0.5 cm) followed by solvent evaporation in the dark for 24 h. Finally, the dry film was hot-pressed at 110 °C to form a uniform film in white color. Other films were prepared through the same method.

Writing and Erasing. When the PCDA/PPC film in white color was irradiated by UV light (365 nm) with an intensity of 60 mW/cm^2 for 60 s, dark blue color arose in the exposed area due to the polymerization of PCDA. The large contrast between white and dark blue colors allowed for information writing with a photomask. In addition, the written information could be erased by flood UV exposure in which all PCDA monomers were converted to PDA. Upon heating to 110 °C, the blue color of PDA/PPC films completely turned to bright red. Additionally, the bright red color could change back to dark blue again upon exposure to 365 nm light. The color change between dark blue and bright red was reversible which allowed for the rewriting by UV irradiation and erasing by heating.

■ ASSOCIATED CONTENT

Supporting Information

The Supporting Information is available free of charge at https://pubs.acs.org/doi/10.1021/acssuschemeng.1c00181.

Topo-polymerization behaviors and variable temperature FTIR spectra of PCDA/PPC and PCDA/PBS films or solutions; UV−vis spectra and temperature of PDA/PPC films under UV irradiation; reversible chromatic switch of PDA, PDA/PBS, and PDA/PPC films; a comparison of light rewritable materials; fluorescence and Raman spectra of PCDA/PPC films; and DSC and TGA curves of PPC or PBS films with varying contents of PDA or PCDA (PDF)

■ AUTHOR INFORMATION

Corresponding Authors

Mingli Ni − *Key Lab for Material Chemistry of Energy Conversion and Storage, Ministry of Education, School of Chemistry and Chemical Engineering, Huazhong University of Science and Technology, Wuhan 430074, China*; Email: mlni@hust.edu.cn

Haiyan Peng − *Key Lab for Material Chemistry of Energy Conversion and Storage, Ministry of Education, School of Chemistry and Chemical Engineering, Huazhong University of Science and Technology, Wuhan 430074, China*; orcid.org/0000-0002-0083-8589; Email: hypeng@hust.edu.cn

Authors

Zhenni Zhou − *Key Lab for Material Chemistry of Energy Conversion and Storage, Ministry of Education, School of Chemistry and Chemical Engineering, Huazhong University of Science and Technology, Wuhan 430074, China*

Wei Wei − *Key Lab for Material Chemistry of Energy Conversion and Storage, Ministry of Education, School of Chemistry and Chemical Engineering, Huazhong University of Science and Technology, Wuhan 430074, China*

Song Li − *State Key Lab of Coal Combustion, School of Energy and Power Engineering, Huazhong University of Science and Technology, Wuhan 430074, China*

Yue Zhang − *Key Lab for Material Chemistry of Energy Conversion and Storage, Ministry of Education, School of Chemistry and Chemical Engineering, Huazhong University of Science and Technology, Wuhan 430074, China*

Qingying Yao − *Key Lab for Material Chemistry of Energy Conversion and Storage, Ministry of Education, School of Chemistry and Chemical Engineering, Huazhong University of Science and Technology, Wuhan 430074, China*

Xingping Zhou − *Key Lab for Material Chemistry of Energy Conversion and Storage, Ministry of Education, School of Chemistry and Chemical Engineering, Huazhong University of Science and Technology, Wuhan 430074, China*

Xiaolin Xie − *Key Lab for Material Chemistry of Energy Conversion and Storage, Ministry of Education, School of Chemistry and Chemical Engineering, Huazhong University of Science and Technology, Wuhan 430074, China*; orcid.org/0000-0001-5097-7416

Complete contact information is available at: https://pubs.acs.org/10.1021/acssuschemeng.1c00181

Author Contributions

Z.N.Z., M.L.N., Y.Z., and Q.Y.Y. conducted the experiments. W.W. and S.L. implemented the computation. H.Y.P. and X.P.Z. instructed the research and discussed the results. Z.N.Z., S.L., M.L.N., H.Y.P., and X.L.X. prepared the manuscript. All authors contributed to writing of the manuscript.

https://doi.org/10.1021/acssuschemeng.1c00181
ACS Sustainable Chem. Eng. 2021, 9, 5902−5909

Notes

The authors declare no competing financial interest.

■ ACKNOWLEDGMENTS

The authors acknowledge the financial supports from NSFC (51773073, 52073108, 51903097) and the Fundamental Research Funds for the Central Universities (2019kfyRCPY089). Technical assistances from the HUST Analytical and Testing Center and Miss Min Lei at the Core Facilities of Life & Sciences (HUST) are gratefully appreciated.

■ REFERENCES

(1) Han, T.; Deng, H.; Qiu, Z.; Zhao, Z.; Zhang, H.; Zou, H.; Leung, N. L. C.; Shan, G.; Elsegood, M. R. J.; Lam, J. W. Y.; Tang, B. Z. Facile Multicomponent Polymerizations toward Unconventional Luminescent Polymers with Readily Openable Small Heterocycles. *J. Am. Chem. Soc.* **2018**, *140*, 5588−5598.

(2) Liu, X.; Li, M.; Han, T.; Cao, B.; Qiu, Z.; Li, Y.; Li, Q.; Hu, Y.; Liu, Z.; Lam, J. W. Y.; Hu, X.; Tang, B. Z. In Situ Generation of Azonia-Containing Polyelectrolytes for Luminescent Photopatterning and Superbug Killing. *J. Am. Chem. Soc.* **2019**, *141*, 11259−11268.

(3) Hu, Y. X.; Hao, X. T.; Xu, L.; Xie, X. L.; Xiong, B. J.; Hu, Z. B.; Sun, H. T.; Yin, G. Q.; Li, X. P.; Peng, H. Y.; Yang, H. B. Construction of Supramolecular Liquid-Crystalline Metallacycles for Holographic Storage of Colored Images. *J. Am. Chem. Soc.* **2020**, *142*, 6285−6294.

(4) Ni, M. L.; Peng, H. Y.; Liao, Y. G.; Yang, Z. F.; Xue, Z. F.; Xie, X. L. 3D Image Storage in Photopolymer/ZnS Nanocomposites Tailored by "Photoinitibitor". *Macromolecules* **2015**, *48*, 2958−2966.

(5) Zhao, X. Y.; Sun, S. S.; Zhao, Y.; Liao, R.-Z.; Li, M.-D.; Liao, Y. G.; Peng, H. Y.; Xie, X. L. Effect of Ketyl Radical on the Structure and Performance of Holographic Polymer/Liquid-Crystal Composites. *Sci. China Mater.* **2019**, *62*, 1921−1933.

(6) Zhao, Y.; Zhao, X. Y.; Li, M. D.; Li, Z. A.; Peng, H. Y.; Xie, X. L. Crosstalk-Free Patterning of Cooperative-Thermoresponse Images by the Synergy of the AIEgen with the Liquid Crystal. *Angew. Chem., Int. Ed.* **2020**, *59*, 10066−10072.

(7) Deng, Y.; Liu, Y.; Qian, Y.; Zhang, W.; Qiu, X. Preparation of Photoresponsive Azo Polymers Based on Lignin, a Renewable Biomass Resource. *ACS Sustainable Chem. Eng.* **2015**, *3*, 1111−1116.

(8) Gao, Y.; Jin, Z. Iridescent Chiral Nematic Cellulose Nanocrystal/Polyvinylpyrrolidone Nanocomposite Films for Distinguishing Similar Organic Solvents. *ACS Sustainable Chem. Eng.* **2018**, *6*, 6192−6202.

(9) Wang, Z. P.; Zhang, Z. Z.; Tao, L. Q.; Shen, N. N.; Hu, B.; Gong, L. K.; Li, J. R.; Chen, X. P.; Huang, X. Y. Hybrid Chloroantimonates(III): Thermally Induced Triple-Mode Reversible Luminescent Switching and Laser-Printable Rewritable Luminescent Paper. *Angew. Chem., Int. Ed.* **2019**, *58*, 9974−9978.

(10) Xie, Y.; Meng, Y.; Wang, W. X.; Zhang, E.; Leng, J. S.; Pei, Q. B. Bistable and Reconfigurable Photonic Crystals-Electroactive Shape Memory Polymer Nanocomposite for Ink-Free Rewritable Paper. *Adv. Funct. Mater.* **2018**, *28*, 1802430.

(11) Sun, H.; Liu, S.; Lin, W.; Zhang, K. Y.; Lv, W.; Huang, X.; Huo, F.; Yang, H.; Jenkins, G.; Zhao, Q.; Huang, W. Smart Responsive Phosphorescent Materials for Data Recording and Security Protection. *Nat. Commun.* **2014**, *5*, 3601.

(12) Wang, W. S.; Xie, N.; He, L.; Yin, Y. D. Photocatalytic Colour Switching of Redox Dyes for Ink-Free Light-Printable Rewritable Paper. *Nat. Commun.* **2014**, *5*, 5459.

(13) Sheng, L.; Li, M. J.; Zhu, S. Y.; Li, H.; Xi, G.; Li, Y.-G.; Wang, Y.; Li, Q. S.; Liang, S. J.; Zhong, K.; Zhang, S. X.-A. Hydrochromic Molecular Switches for Water-Jet Rewritable Paper. *Nat. Commun.* **2014**, *5*, 3044.

(14) Khazi, M. I.; Jeong, W.; Kim, J. M. Functional Materials and Systems for Rewritable Paper. *Adv. Mater.* **2018**, *30*, 1705310.

(15) Wegner, G. Tochemical Reactions of Monomers with Conjugated Triple Bonds. *Naturforsch. Teil B* **1969**, *24*, 824−832.

(16) Kootery, K. P.; Jiang, H.; Kolusheva, S.; Vinod, T. P.; Ritenberg, M.; Zeiri, L.; Volinsky, R.; Malferrari, D.; Galletti, P.; Tagliavini, E.; Jelinek, R. Poly(Methyl Methacrylate)-Supported Polydiacetylene Films: Unique Chromatic Transitions and Molecular Sensing. *ACS Appl. Mater. Interfaces* **2014**, *6*, 8613−8620.

(17) Peng, H. S.; Tang, J.; Pang, J. B.; Chen, D. Y.; Yang, L.; Ashbaugh, H. S.; Brinker, C. J.; Yang, Z. Z.; Lu, Y. F. Polydiacetylene/Silica Nanocomposites with Tunable Mesostructure and Thermochromatism from Diacetylenic Assembling Molecules. *J. Am. Chem. Soc.* **2005**, *127*, 12782−12783.

(18) Okaniwa, M.; Oaki, Y.; Imai, H. Intercalation-Induced Tunable Stimuli-Responsive Color-Change Properties of Crystalline Organic Layered Compound. *Adv. Funct. Mater.* **2016**, *26*, 3463−3471.

(19) Park, D.-H.; Jeong, W.; Seo, M.; Park, B. J.; Kim, J.-M. Inkjet-Printable Amphiphilic Polydiacetylene Precursor for Hydrochromic Imaging on Paper. *Adv. Funct. Mater.* **2016**, *26*, 498−506.

(20) Wang, X. N.; Sun, X. L.; Hu, P. A.; Zhang, J.; Wang, L. F.; Feng, W.; Lei, S. B.; Yang, B.; Cao, W. W. Colorimetric Sensor Based on Self-Assembled Polydiacetylene/Graphene-Stacked Composite Film for Vapor-Phase Volatile Organic Compounds. *Adv. Funct. Mater.* **2013**, *23*, 6044−6050.

(21) Ahn, D. J.; Chae, E. H.; Lee, G. S.; Shim, H. Y.; Chang, T. E.; Ahn, K. D.; Kim, J. M. Colorimetric Reversibility of Polydiacetylene Supramolecules Having Enhanced Hydrogen-Bonding under Thermal and pH Stimuli. *J. Am. Chem. Soc.* **2003**, *125*, 8976−8977.

(22) Phollookin, C.; Wacharasindhu, S.; Ajavakom, A.; Tumcharern, G.; Ampornpun, S.; Eaidkong, T.; Sukwattanasinitt, M. Tuning Down of Color Transition Temperature of Thermochromically Reversible Bisdiynamide Polydiacetylenes. *Macromolecules* **2010**, *43*, 7540−7548.

(23) Heo, J.-M.; Son, Y.; Han, S.; Ro, H.-J.; Jun, S.; Kundapur, U.; Noh, J.; Kim, J.-M. Thermochromic Polydiacetylene Nanotube from Amphiphilic Macrocyclic Diacetylene in Aqueous Solution. *Macromolecules* **2019**, *52*, 4405−4411.

(24) Oh, S.; Uh, K.; Jeon, S.; Kim, J.-M. A Free-Standing Self-Assembled Tubular Conjugated Polymer Sensor. *Macromolecules* **2016**, *49*, 5841−5848.

(25) Xu, Y.-Y.; Ding, Z.-F.; Liu, F.-Y.; Sun, K.; Dietlin, C.; Lalevée, J.; Xiao, P. 3D Printing of Polydiacetylene Photocomposite Materials: Two Wavelengths for Two Orthogonal Chemistries. *ACS Appl. Mater. Interfaces* **2020**, *12*, 1658−1664.

(26) Peng, H.; Tang, J.; Yang, L.; Pang, J.; Ashbaugh, H. S.; Brinker, C. J.; Yang, Z.; Lu, Y. Responsive Periodic Mesoporous Polydiacetylene/Silica Nanocomposites. *J. Am. Chem. Soc.* **2006**, *128*, 5304−5305.

(27) Kim, J.-M.; Lee, J.-S.; Choi, H.; Sohn, D.; Ahn, D. J. Rational Design and in-Situ FTIR Analyses of Colorimetrically Reversibe Polydiacetylene Supramolecules. *Macromolecules* **2005**, *38*, 9366−9376.

(28) Yao, Y.; Dong, H.; Liu, F.; Russell, T. P.; Hu, W. Approaching Intra- and Interchain Charge Transport of Conjugated Polymers Facilely by Topochemical Polymerized Single Crystals. *Adv. Mater.* **2017**, *29*, 1701251.

(29) Jeong, W.; Khazi, M. I.; Lee, D. G.; Kim, J.-M. Intrinsically Porous Dual-Responsive Polydiacetylenes Based on Tetrahedral Diacetylenes. *Macromolecules* **2018**, *51*, 10312−10322.

(30) Zhu, L. L.; Tran, H.; Beyer, F. L.; Walck, S. D.; Li, X.; AÅgren, H.; Killops, K. L.; Campos, L. M. Engineering Topochemical Polymerizations Using Block Copolymer Templates. *J. Am. Chem. Soc.* **2014**, *136*, 13381−13387.

(31) Sakakura, T.; Choi, J.-C.; Yasuda, H. Transformation of Carbon Dioxide. *Chem. Rev.* **2007**, *107*, 2365−2387.

(32) Wang, Y.; Zhao, Y. J.; Ye, Y. S.; Peng, H. Y.; Zhou, X. P.; Xie, X. L.; Wang, X. H.; Wang, F. S. A One-Step Route to CO_2-Based Block Copolymers by Simultaneous ROCOP of CO_2/Epoxides and RAFT Polymerization of Vinyl Monomers. *Angew. Chem., Int. Ed.* **2018**, *57*, 3593−3597.

(33) Zeng, B.; Li, Y.; Wang, L.; Zheng, Y.; Shen, J.; Guo, S. Body Temperature-Triggered Shape-Memory Effect Via Toughening Sustainable Poly(Propylene Carbonate) with Thermoplastic Polyurethane: Toward Potential Application of Biomedical Stents. *ACS Sustainable Chem. Eng.* **2020**, *8*, 1538−1547.

https://doi.org/10.1021/acssuschemeng.1c00181
ACS Sustainable Chem. Eng. 2021, 9, 5902−5909

(34) Li, W.; Qin, J.; Wang, S.; Han, D.; Xiao, M.; Meng, Y. Macrodiols Derived from CO_2-Based Polycarbonate as an Environmentally Friendly and Sustainable PVC Plasticizer: Effect of Hydrogen-Bond Formation. *ACS Sustainable Chem. Eng.* **2018**, *6*, 8476−8484.
(35) Biradha, K.; Santra, R. Crystal Engineering of Topochemical Solid State Reactions. *Chem. Soc. Rev.* **2013**, *42*, 950−967.
(36) Matsumoto, A.; Tanaka, T.; Tsubouchi, T.; Tashiro, K.; Saragai, S.; Nakamoto, S. Crystal Engineering for Topochemical Polymerization of Muconic Esters Using Halogen-Halogen and CH/π Interactions as Weak Intermolecular Interactions. *J. Am. Chem. Soc.* **2002**, *124*, 8891−8902.
(37) Tahir, M. N.; Nyayachavadi, A.; Morin, J.-F.; Rondeau-Gagné, S. Recent Progress in the Stabilization of Supramolecular Assemblies with Functional Polydiacetylenes. *Polym. Chem.* **2018**, *9*, 3019−3028.
(38) Zhang, D.-D.; Ruan, Y.-B.; Zhang, B.-Q.; Qiao, X.; Deng, G.; Chen, Y.; Liu, C.-Y. A Self-Healing PDMS Elastomer Based on Acylhydrazone Groups and the Role of Hydrogen Bonds. *Polymer* **2017**, *120*, 189−196.
(39) Hasegawa, M. Photopolymerization of Diolefin Crystals. *Chem. Rev.* **1983**, *83*, 507−518.
(40) Jorgensen, W. L.; Maxwell, D. S.; Tirado-Rives, J. Development and Testing of the OPLS All-Atom Force Field on Conformational Energetics and Properties of Organic Liquids. *J. Am. Chem. Soc.* **1996**, *118*, 11225−11236.
(41) Wang, J.; Wolf, R. M.; Caldwell, J. W.; Kollman, P. A.; Case, D. Development and Testing of a General Amber Force Field. *J. Comput. Chem.* **2004**, *25*, 1157−1174.
(42) Stroet, M.; Caron, B.; Visscher, K. M.; Geerke, D. P.; Malde, A. K.; Mark, A. E. Automated Topology Builder Version 3.0: Prediction of Solvation Free Enthalpies in Water and Hexane. *J. Chem. Theory Comput.* **2018**, *14*, 5834−5845.
(43) Frisch, M. J.; Schlegel, H. B.; Scuseria, G. E.; Robb, M. A.; Scalmani, G., Barone, V.; Mennucci, B.; Petersson, G. A.; Caricato, M.; Li, X.; Hratchian, H. P.; Izmaylov, A. F.; Zheng, G.; Sonnenberg, J. L.; Hada, M.; Ehara, M.; Fukuda, R.; Hasegawa, J.; Ishida, M.; Nakajima, T.; Honda, Y.; Nakai, H.; Vreven, T.; Montgomery, Jr., J. A.; Peralta, J. E.; Bearpark, M.; Heyd, J. J.; Brothers, E.; Kudin, K. N.; Keith, T.; Kobayashi, R.; Normand, J.; Raghavachari, K.; Burant, J. C.; Iyengar, S. S.; Tomasi, J.; Cossi, M.; Millam, J. M.; Klene, M.; Knox, J. E.; Cross, J. B.; Bakken, V.; Jaramillo, J.; Gomperts, R.; Stratmann, R. E.; Yazyev, O.; Cammi, R.; Pomelli, C.; Ochterski, J. W.; Martin, R. L.; Zakrzewski, V. G.; Voth, G. A.; Salvador, P.; Dapprich, S.; Daniels, A. D.; Farkas, O.; Ortiz, J. V.; Cioslowski, J.; Fox, D. J. *Gaussian 09, Revision D.01*; Gaussian, Inc.: Wallingford CT, 2013.
(44) Salomon-Ferrer, R.; Case, D. A.; Walker, R. C. An Overview of the Amber Biomolecular Simulation Package. *WIREs Comput. Mol. Sci.* **2013**, *3*, 198−210.
(45) Hess, B.; Kutzner, C.; Spoel, D. v. d.; Lindahl, E. Algorithms for Highly Efficient, Load-Balanced, and Scalable Molecular Simulation. *J. Chem. Theory Comput.* **2008**, *4*, 435−447.
(46) Essmann, U.; Perera, L.; Berkowitz, M. L.; Darden, T.; Lee, H.; Pedersen, L. G. A Smooth Particle Mesh Ewald Method. *J. Chem. Phys.* **1995**, *103*, 8577−8593.
(47) Deshmukh, S. A.; Sankaranarayanan, S. K.; Suthar, K.; Mancini, D. C. Role of Solvation Dynamics and Local Ordering of Water in Inducing Conformational Transitions in Poly(N-Isopropylacrylamide) Oligomers through the LCST. *J. Phys. Chem. B* **2012**, *116*, 2651−2663.
(48) Spoel, D. v. d.; Maaren, P. J. v.; Larsson, P.; Timneanu, N. Thermodynamics of Hydrogen Bonding in Hydrophilic and Hydrophobic Media. *J. Phys. Chem. B* **2006**, *110*, 4393−4398.

https://doi.org/10.1021/acssuschemeng.1c00181
ACS Sustainable Chem. Eng. 2021, 9, 5902−5909